Dalton Transactions

Accepted Manuscript

ROYAL SOCIETY OF CHEMISTRY

www.rsc.org/dalton

Cite this: DOI: 10.1039/c0xx00000x

www.rsc.org/xxxxxx

ARTICLE TYPE

Designed synthesis of CO_2 promoted copper(II) coordination polymers: synthesis, structural, spectroscopic characterization and versatile functional property studies†

Pritam Ghosh,[a] Additi Roychowdhury,[ab] Montserrat Corbella,[c] Asim Bhaumik,[d] Partha Mitra,[d] Shaikh M. Mobin,[e] Ayan Mukherjee,[f] Soumen Basu,[f] and Priyabrata Banerjee*[ab]

Received (in XXX, XXX) Xth XXXXXXXXX 20XX, Accepted Xth XXXXXXXXX 20XX
DOI: 10.1039/b000000x

A series of CO_2 promoted Cu(II) coordination polymers in different coordination environments have been synthesized. The molecular description as well as properties of the four complexes has been investigated by CHN, MS, UV-VIS, IR, PXRD, TEM, SQUID,SC-XRD, NLDFT and electrical property characterizations. Single crystal X-ray structure determination of $[Cu(bpy)(C_2O_4)]_n$ (**1**) and $[Cu(2\text{-}AMP)_2(C_2O_4)]_n$ (**2**) depicts their polynuclearity [bpy = 2,2'-bipyridine, 2-AMP = 2-amino pyridine; 2-AMP is a cleaved ligand of starting ligand $\mathbf{L^1}$ = N-(phenyl(pyridin-2-ylamino)methyl)pyridin-2-amine]. Both the complexes have distorted octahedral geometry. Starting from an another tripodal ligand $\mathbf{L^2}$ [$\mathbf{L^2}$ = 2-(((2-(pyridin-2-yl)ethyl)(pyridin-2-ylmethyl)amino)methyl)phenol, $\mathbf{L^{2\prime}}$ (cleaved L^2 ligand) = 2-(pyridin-2-yl)-N-((pyridin-2-yl)methyl)ethanamine], a mononuclear complex $[Cu(L^2)(Cl)]$ (**3**) has been obtained with a distorted square pyramidal geometry. Polynuclear complexes **1, 2** and **4** are CO_2 mediated functional materials which have been produced in benzonitrile solvent medium. Interestingly complex **4** of cleaved $\mathbf{L^2}$ ligand is an wonderful copper based functional material with appreciable surface area. Powder XRD and TEM analysis of complex **4** supports its mesoporosity. Moreover all the four complexes act as semiconductor over a wide temperature range.

Introduction

In the modern age, global warming has resulted due to the key factors of uncontrolled burning of fossil fuel and excessive deforestation. CO_2 is known to be one of the biggest contributing partners of green house gas (GHG) family, has to be checked, keeping in mind its major contribution in global warming. Extensive research works in this respect is taking place worldwide to reduce the concentration of CO_2 from air. In this regard very cheap, safe and easy to perform technique for fixation of CO_2 using suitable transition metal complex is a promising approach for utilization of CO_2 as raw material for preparing useful chemical feedstock.[1] Mankind can be benefitted hugely in the future if CO_2 can be utilized as a raw material for production of robust functional material. A viable approach in carbon dioxide inclusion chemistry is the reduction of CO_2 in presence of suitable coordination complexes.[1c] Electrochemical reduction of electroactive materials on metal electrodes generally requires higher negative electrode potentials.[2] The one electron reduction of CO_2 to $[CO_2^{\bullet}]^-$ generally occurs at very high potential of -2.21 eV *vs* SCE.[3] For conversion and ligation of CO_2 into metal centre it is always important to reduce its potential as much as possible and in doing so the main engineering is lying in the selection of properly chosen catalyst which can facilitate its reduction. Use of transition metal complexes as electrocatalyst towards the reduction reaction generally occurs at lower negative potential.[4] Direct CO_2 incorporated useful chemical feedstock *via* transition metal complex mediation has hitherto been very less explored. Our concern is to understand the CO_2 inclusion chemistry[3] in presence of low cost copper complexes and suitable solvent medium as catalyst.

In this present work our aim is to investigate CO_2 mediated reaction chemistry of several low cost copper complex precursors having redox active organic co-ligands as electron reservoir towards catalytic reaction. Reductive coupling of CO_2 molecules leads to oxalato bridged robust copper coordination polymers. Notably these coordination polymers have potential electrical conducting property.

Results and discussion

Synthesis and Characterization

The reaction of anhydrous $CuCl_2$ with bpy (1:1) in benzonitrile medium with CO_2 purging at room temperature yields upon the complex $[Cu(bpy)(C_2O_4)]_n$ (**1**). Reductive coupling of CO_2 to form oxalate dianion ($C_2O_4^{2-}$) may occur either *via* outersphere pathway using mercury or lead electrodes for electrocatalysis or *via* innersphere pathways using transition metal complex or anion radicals of aromatic hydrocarbons.[3]

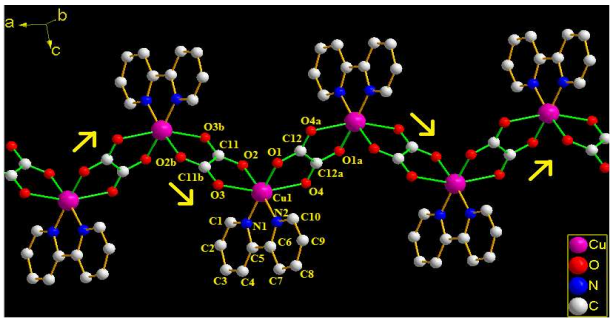

Fig. 1 Molecular view of the complex **1.** Hydrogen atoms are omitted for clarity. 1D chain propagation is directed by yellow arrow. Selected bond distances (Å) and angles (°) are given in Table S1, ORTEP is shown in Fig. S1 (ESI†).

In this case in presence of benzonitrile as catalyst,[5] bpy acts as electron reservoir for the conversion of CO_2 to $C_2O_4^{2-}$. Gas

flowing in presence of bpy first initiate $1e^-$ reduction of $[CO_2]$ to form $[CO_2^{\bullet}]^-$ which on further dimerisation form $[C_2O_4]^{2-}$ due to the close proximity of $[CO_2^{\bullet}]^-$ species in starting Cu-bpy complex solution mixture, resulting formation of a 1D polynuclear chain $[Cu(bpy)(C_2O_4)]_n$ (**1**) (Fig. 1).[6] We also perform the same reaction in presence of PPh_3 as a good σ donor to make the reaction more facile towards CO_2 incorporation. Unfortunately in presence of PPh_3 the yield of the reaction is even less (*ca.* 25%) rather than it is enhanced. Here, PPh_3 is directly participating in the reaction solution by forming $[Cu(bpy)(PPh_3)_2]ClO_4$ (**1'**) which is confirmed by ESI-MS, ORTEP and FT-IR studies (see, Fig. S2, S3 and S11,Table S5, ESI†).

After picturing the Cu-bpy solution chemistry over CO_2 we are interested with another N, N donor synthesized ligand $\mathbf{L^1}$ (N-(phenyl(pyridin-2-ylamino)methyl)pyridin-2-amine).[7]The molecular view of the ligand is shown in Fig. 2.

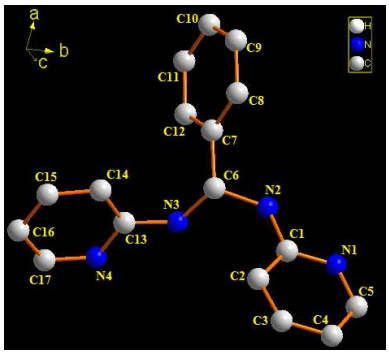

Fig. 2 Molecular view of the ligand $\mathbf{L^1}$ [H atoms are omitted for clarity]. Selected bond distances (Å) and angles (°) are given in supporting Table S2, ORTEP is shown in Fig. S4 (ESI†).

An interesting result is obtained when we start with same starting material, anhydrous cupric chloride in presence of ligand $\mathbf{L^1}$ in benzonitrile medium at room temperature in O_2 free CO_2 atmosphere, where CO_2 purging was continued for ~ 0.5 h. C-N bond activation followed by C-N bond clevage reaction takes place in the ligand backbone[8] and CO_2 promoted another complex $[Cu(2\text{-}AMP)_2(C_2O_4)]_n$ (**2**) is formed (Fig. 3). Once again CO_2 to $C_2O_4^{2-}$ formation occurs where the truncated amino pyridine coligand working as an electron reservoir in presence of benzonitrile solvent as a catalyst in this whole transformation and produces $[Cu(2\text{-}AMP)_2(C_2O_4)]_n$ (**2**).

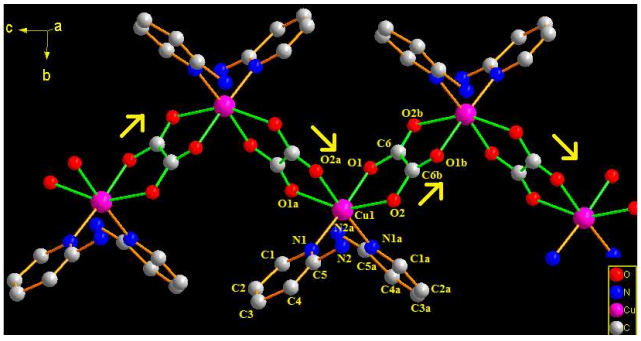

Fig. 3 Molecular view of the complex **2.** Hydrogen atoms are omitted for clarity. 1D chain propagation is directed by yellow arrow. Selected bond distances (Å) and angles (°) are given in supporing Table S3, ORTEP is shown in Fig. S5 (ESI†).

Apart from bpy and a cleaved ligand of $\mathbf{L^1}$ containing Cu-coordination polymer, another CO_2 incorporated polymeric copper complex was also synthesized starting from a mononuclear copper complex $[Cu(L^2)(Cl)]$ (**3**) (Fig. 4). The tripodal ligand $\mathbf{L^2}$ [2-(((2-(pyridin-2-yl)ethyl)(pyridin-2-ylmethyl)amino)methyl)phenol] was synthesized by literature method.[9] For betterment of yield we always added 2-chloromethyl pyridine hydrochloride in excess.[9b] CO_2 mediated reaction of mononuclear tripodal copper complex **3** in benzonitrile at room temperature will result an oxalato bridged Cu-dinuclear complex **4** containing cleaved $\mathbf{L^2}$ ligand, $\mathbf{L^{2\prime}}$ = 2-(pyridin-2-yl)-N-((pyridin-2-yl)methyl)ethanamine. Herein CO_2 to $C_2O_4^{2-}$ are formed in presence of several heterocyclic aromatic rings of $\mathbf{L^2}$. These aromatic rings are working as electron reservoir similar to co-ligands of **1** and **2** in similar solvent medium for insitu oxalate generation. The di-nuclear oxalato bridged copper complex resulted in dissociation of one of its side arm in ligated $\mathbf{L^2}$ due to JT distortion of copper(II) d^9 system. We were not fortunate enough to grow single crystal of dinuclear complex **4**.

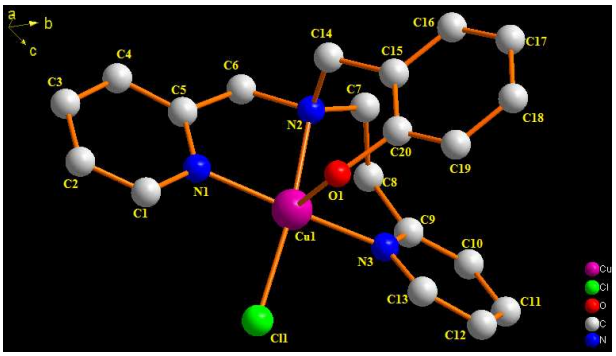

Fig. 4 Molecular view of the complex **3.** Hydrogen atoms are omitted for clarity. Selected bond distances (Å) and angles (°) are given in supporing Table S4, ORTEP is shown in Fig. S6a (ESI†).

However from solid as well as solution state material chracterisation tools like FT-IR, Magnetic study, elemental analysis, FAB and ESI–MS study we are confirmed regarding its formation. [see, Fig. 5 and 9 (*infra*), Fig. S7-S8, Table S6 ESI†]. Moreover, TEM and sorption studies have shown it's mesoporous nature with interesting sorption properties within it.[10]

1 and **2** both are distorted octahedral in nature (Table S5, ESI†). A mononuclear tripodal complex of Cu(II) (**3**) having square pyramidal geometry is formed around central Cu^{II} atom where a Cl atom and three nitrogen atoms from L^2 (two nitrogen atoms from two pyrido side arms and one central nitrogen) form the base of the pyramid with the O atom occupying the apical position. This type of geometry can be assigned based on the τ factors defined by Reedijk *et al.*[11] τ = 0 for a perfect square pyramidal geometry and τ = 1 for trigonal bipyramidal structure (here τ = 0.068, less distorted square pyramidal geometry).

A schematic representation of all the CO_2 promoted reactions starting from simple anhydrous $CuCl_2$ with different co-ligands are depicted in scheme 1:

FT-IR Study

IR spectra of all the polynuclear Cu(II) coordination complexes shows the presence of all characteristics bands for coorinated ligands with $\upsilon_{C\text{-}N}$,$\upsilon_{C=C}$ appearing in the ranges 1590-1640 and

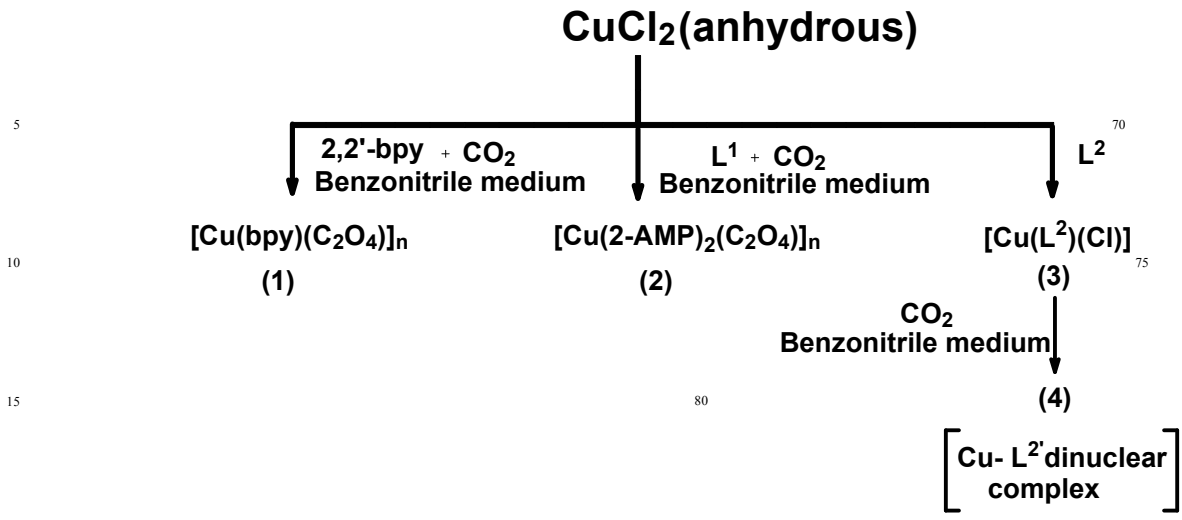

Scheme 1 CO_2 promoted polynuclear complex fabrication.

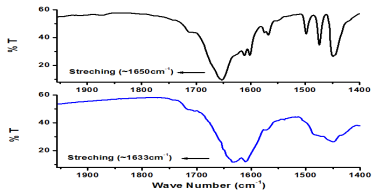

Fig. 5 Overlayed FT-IR spectra of the representative complex **1** (black) and **4** (blue).

1400-1600 cm^{-1} respectively. The characteristic streching frequencies of $C_2O_4^{2-}$are coming in the expected region of 1630-1665 cm^{-1} for complexes **1**, **2** and **4**.[12a] Here we are showing IR for **1** and **4** in Fig. 5. The stretching of C_2O_4 group in case of complex **4** is coming at ~1633cm^{-1},[12b] which bolster our prediction about fixation of CO_2 in form of C_2O_4 at complex **4** (further supported by FAB and ESI-MS and magnetic measurement data in favour of CO_2 ligation in the form of $C_2O_4^{2-}$; *vide* Fig. S7-S8 ESI†, Fig. 9). A detailed description of IR studies are described in supporting information (see, Fig. S9-S11 and frequency details (ν, cm^{-1}) in text ESI†).

Powder XRD study

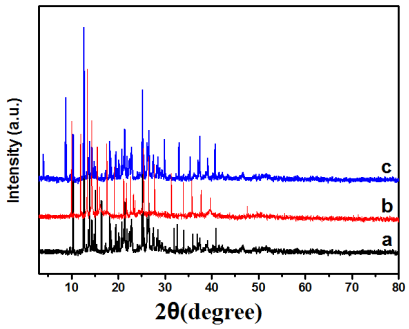

Fig. 6 Powder XRD patterns of (**a**) **1**, (**b**) **2** and (**c**) **4**.

Small angle X-ray Powder diffraction studies do not show any powder diffraction characteristics of mesoporous material for complex **1** and **2**. For complex **4** high intensity diffraction peak was observed (Fig. 6), which reflects ordered meso and very small micro structure in this material.[13] Some sort of loss of crystallinity observed with a slight shift of peak to the low angle(2θ) implies the presence of porosity in **4**. Quadrupolar interaction of CO_2 with the unsaturated Cu centre may be the driving force for the formation of such porous complex.

Nanostructure and porosity studies

In Fig. 7a HR TEM image of the representative complex **4** is shown. As seen from these images that the complex is composed of very tiny nanoparticles of dimension *ca.* 12-15 nm. Low electron density white spots or pores at the interparticle spaces of dimensions *ca*. 4-5 nm are seen throughout the specimen. SAED pattern shown in Fig. 7b suggest that there are diffraction spots corresponding to the crystalline planes. Adsorption/desorption

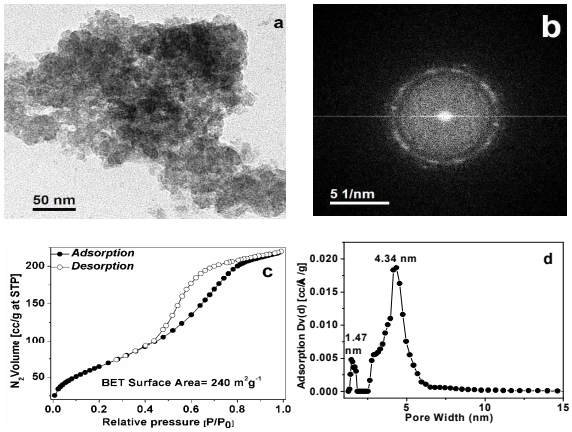

Fig. 7a Transmission electron micrograph of **4**. **Fig. 7b** SAED pattern of as synthesized **4**. **Fig. 7c** N_2 sorption/desorption isotherm of **4**. Adsorption points are marked by filled symbols and desorption points by empty symbols. Pore size distribution of **4** is shown in **Fig. 7d.**

isotherm of the complex **4** is shown in Fig. 7c. This isotherm can be classified as type IV corresponding to those of mesoporous materials.[14] From the N_2 sorption isotherms the BET surface area for **4** is found to be 240 m^2g^{-1} and a total pore volume of 0.318 cm^3g^{-1}. Pronounced desorption hysteresis suggests the existence of large mesopores in this material. This hysteresis is an intermediate between typical H1 and H2-type hysteresis loop, which originates in the P/P_0 range from 0.50 to 0.85. This result suggests that large uniform mesopores with a cage like pore

structure could exist.[15] Pore size distribution of **4** employing non local density functional theory (NLDFT) is shown in Fig. 7d. An observed peak maximum from this isotherm was at 4.34 nm. Interparticle porosity could be the origin of this mesopores.[14] Pore width at around 1.47 nm is responsible for its microporous feature which can also be discernible at very low relative pressure in the nitrogen adsorption/desorption isotherm ($P/P_0 < 0.01$) (Fig. 7c).

Magnetic study

The metal complexes **1**, **2** and **4** are the end product of CO_2 inclusion reaction. Though Cu(II) polynuclear chains are not very prospective candidate from magneto chemical point of view, but as these coordination polymers have been produced as a result of CO_2 inclusion chemistry, it is always interesting to observe the effect of bridging C_2O_4 at each paramagnetic Cu(II) centre of **1**, **2** and **4**. Magnetic properties of **1** and **2** are shown as $\chi_M T$ *vs T* plot in Fig. 8 (the magnetic data are reported for one Cu ion). At room temperature the $\chi_M T$ value is ~0.40 cm^3 mol^{-1} K, for both complexes, which is close to the expected magnetic moment for one uncoupled Cu(II) ion. This value remains practically constant upon cooling until ~60 K and further increases continuously to reach 0.78 cm^3 mol^{-1} K, for **1** and 0.62 cm^3 mol^{-1} K, for **2** at 2 K. This behaviour is characteristic of a ferromagnetic interaction between the Cu(II) ions in the one dimensional system. The experimental $\chi_M T$ data were analysed with the numerical expression proposed by Baker and Rushbrooke[16] for a ferromagnetic uniform chain:

$\chi_M T = (Ng^2\beta^2/4k)/(\ 1.0+5.7979916\ x+16.902653\ x^2\ +29.376885\ x^3+29.832959\ x^4+14.036918\ x^5)/(\ 1.0+2.7979916x+7.0086780\ x^2+8.6538644\ x^3+4.5743114\ x^4))^{2/3}$

where x =J/kT. Least-squares fit of the experimental data lead to the following values J =+0.77 cm^{-1}, g = 2.09 and $R = 9.10\text{x}10^{-5}$ for **1** and J = +0.44 cm^{-1}, g = 2.07 and $R = 1.62\text{x}10^{-4}$ for **2**.

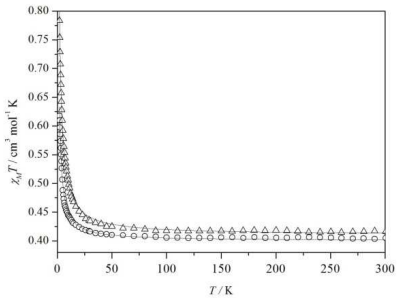

Fig. 8 Plot of the thermal variation of $\chi_M T$ *vs T* for **(1)** (Δ) and (**2**) (O). The solid lines are the best fit to the experimental data.

The ferromagnetic coupling found in **1** and **2** are weak in nature and correspond to a case of accidental orthogonality between the interacting magnetic orbitals through the out-of-plane exchange pathway. The Cu(II) ions show an elongated coordination octahedral, with a parallel disposition of the Jahn-Teller axes along the chain. The unpaired electron on each Cu(II) ion is located in a d_{x2-y2} type metal centered magnetic orbital [the x and y axes being roughly defined by the Cu-N bonds] which is positioned in the equatorial plane and the two magnetic orbitals are parallel to each other and perpendicular to the C_2O_4 plane of the octahedra (scheme 2). According to the Khan's model[17] the magnetic coupling constant J has two contributions, a ferromagnetic contribution (J_F) and an antiferromagnetic contribution (J_{AF}) that depends on the overlap between the

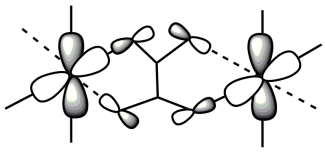

Scheme 2 A schematic representation of the interaction between the magnetic orbitals in the C_2O_4-bridged Cu(II) fragments of **1** and **2**.

magnetic orbitals. For complexes **1** and **2**, due to the parallel disposition of the magnetic orbitals, the antiferromagnetic contribution could be negligible and a weak ferromagnetic behavior is observed. Several C_2O_4-bridged Cu(II) complexes having the out-of-plane exchange pathway have been reported in the literature; Table 1 collects the magneto-structural data of these complexes. Analogous complexes to **1** and **2** have also been reported in the literature,[18,19] however, due to the different synthetic route these complexes show small structural differences, that influence to the magnetic coupling. Complexes **1** and **2** show weaker ferromagnetic coupling than the analogous compounds reported in the literature. $\chi_M T$ *vs T* plot for complex **4** is shown in Fig. 9 (the magnetic data are reported for one Cu ion). At room temperature the $\chi_M T$ value is ~0.40 cm^3 mol^{-1} K, close to the expected value for one uncoupled Cu(II) ion. This value remains practically constant upon cooling until ~30 K and further decreases continuously to reach 0.26 cm^3 mol^{-1} K at 2 K. This behaviour is characteristic of an antiferromagnetic interaction between the Cu(II) ions, and suggests the presence of a bridging ligand between the Cu(II) ions. The experimental data fit well with the equation of Bonner and Fisher[26] for a one-dimensional system with antiferromagnetic coupling: $\chi_M T=(Ng^2\beta^2/k)/((0.25+0.074975x+0.075235x^2)/(1.0+0.9931x+0.172135x^2+0.757825x^3))$ where $x = |J|/kT$. Least-squares fit of the experimental data lead to the following values J = -1.04 cm^{-1}, g = 2.11 and $R = 3.04\text{x}10^{-5}$.

The weak antiferromagnetic interaction suggests a parallel disposition of the two Cu-centered magnetic orbital's which are perpendicular to the C_2O_4 bridging ligand. Unfortunately, it was not possible to obtain enough quantity of pure compound of **3** to measure the magnetic data. However, the crystal structure of this compound shows a mononuclear complex with distances between two neighboring Cu(II) ions of 4.5 Å and the distance of one Cu(II) ion and the Cl ligand of the other entity is 3.7 Å. These data suggest that the magnetic interaction between the mononuclear complexes could be expected to be negligible.

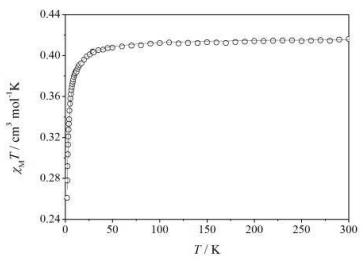

Fig. 9 Plot of the thermal variation of $\chi_M T$ *vs T* for **4**. The solid line is the best fit to the experimental data.

Complexes[a]	*d(Cu-O$_{ax}$)*[b] *Å*	*h$_{Cu}$*[c] *Å*	*β*[d] *deg*	*γ*[e] *deg*	*d(Cu···Cu) Å*	*J cm^{-1}*	*references*
$[[Cu(bpy)(C_2O_4)]\cdot 2H_2O]_n$	2.31	0.034	108.3	86.8	5.56	2.4	18
$[[Cu(bpy)(C_2O_4)]\cdot H_2O]_n$	2.31	0.035	108.6	83.8	5.55	0.77	Thiswork
$[Cu(2\text{-}ampy)_2(C_2O_4)]_n$	2.38	0.02	107.8	75.6	5.63	2.0	19
$[Cu(2\text{-}amp)_2(C_2O_4)]_n$	2.39/2.37	0.01	108.8	83.2	5.65	0.44	Thiswork
$[Cu(3\text{-}ampy)_2(C_2O_4)]_n$	2.17	0.0	111.0	85.2	5.46	-1.3	19
$[Cu(4\text{-}ampy)_2(C_2O_4)]_n$	2.35	0.0	109.7	88.7	5.66	-1.1	19
$[Cu(isq)_2(C_2O_4)]_n$	2.23	0.06	109.5	88.5	5.48	0.63	21
$[Cu(py)_2(C_2O_4)]_n$	2.27	0.0	108.0	80.0	5.46	1.4	20
$[(NMe_4)_2[Cu(C_2O_4)_2]\cdot H_2O]_n$	2.38	0.04	106.9	79.1	5.59	1.14	22
$[Cu_2(bpca)_2(C_2O_4)]$	2.26	0.16	107.5	92	5.44	1.1	23
$[Cu_2(bpca)_2(H_2O)_2(C_2O_4)]\cdot 2H_2O$	2.41	0.05	106.9	80.7	5.63	1.0	24
$[Cu_2(bpcam)_2(H_2O)_2(C_2O_4)]$	2.44	0	106.6	101.8	5.68	0.75	25

Table 1 Selected magneto-structural data for C_2O_4-bridged complexes having the out-of-plane exchange pathway

[a]Abbreviations of the ligands: bpy: 2,2-bipyridine; py: pyridine; 2-ampy: 2-aminopyridine; 3-ampy:3-aminopyridine; 4-ampy: 4-aminopyridine;isq: isoquinoline; bpca: bis(2-pyridylcarbonyl)amidate; bpcam: bis(2.pyrimidylcarbonyl)amidate. [b] Value of the axial Copper to oxalate-oxygen.[c] The height of the Cu atom from the equatorial plane.[d] Bond angle at the axial oxalate–oxygen (Cu–O–C).[e] Dihedral angle between the equatorial and C_2O_4 planes.

Electrical Property study

The dc electronic properties of all the CO_2 inclusion polynuclear complexes [**1**, **2** and **4**] along with the mononuclear complex **3** have been measured in the temperature range 298-373 K. Fig. 10a shows the variation in ln ρ(T) with 1000/T. It is evident from the Fig. 10a that all the compounds behave like semi conducting materials *i.e.,* their resistivity decreases with the increase of temperature. The activation energy of all the investigated compound have been estimated by using the Arrhenius equation

$$\rho(T) = \rho_0 e^{Ea/KT}$$

where ρ_0 is the resistivity at infinite temperature, E_a is the activation energy, and k is the Boltzmann constant. The activation energy "E_a" can be calculated from the slopes of the straight line plot of ln ρ(T) with 1/T. For **1** the activation energy is found to be 0.56 eV and for **2** it is 0.04eV where as it is found that there are two different slopes for the **3** and **4**, *i.e* two different activation processes are present in these complexes. The activation energy for lower temperature regions is 1.16 eV for complex **3** and 0.2 eV for complex **4**. On the other hand the activation energy at higher temperature region are 3.35 eV and 1.69 eV for **3** and **4** respectively.

Fig. 10b shows the variation of dielectric permittivity with frequency. The dielectric properties of the compounds have been measured in the frequency range 20 Hz-2MHz at 323 K and found that it depends on both the grain resistance and interfacial grain boundary resistance. It is also observed from the Fig. 10b that the dielectric permittivity is larger at low frequency regions and it decreases at higher frequency regions. This is because at higher frequency regions, the mobility of charge carriers is low and cannot follow the alternation of the applied alternating electric field. A large degree of dispersion occurs because of charge transfer within the interfacial diffusion layers present between the electrodes, confirmed by the sharp increase at low frequencies.

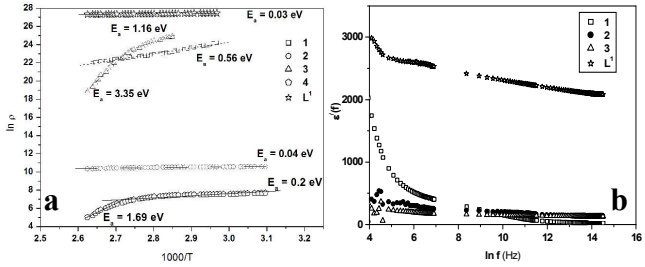

Fig. 10a and **10b.** Conductivity studies of **1**, **2**, **3**, **4** and **L^1**.

Conclusion

In the present work we have unveiled the chemistry of CO_2 promoted reactions of a series of low cost mononuclear copper(II) coordination complexes starting from selectively chosen heterocyclic multidentate ligands. The electrochemical reduction of CO_2 to one e- reduced intermediate $[CO_2^{\bullet}]^-$ requires very large negative potential due to its inertness. The presence of suitable metal complexes in aprotic solvent as electrocatalyst can easily drop down the high negative potential of the redox reaction. Moreover presence of redox non-innocent multidentate ligands as electron reservoir helps insitu $[C_2O_4]^{2-}$ formation from CO_2. Carbon-di-oxide promoted reaction yields upon oxalato bridged polynuclear complexes **1** and **2** and dinuclear complex **4**. The most salient feature is that during CO_2 mediated inclusion reaction, internal electron transfer takes place in the system involving several C-N bond breakings in the co-ligand backbones (L^1 and L^2) as well as bond making *i.e.* dimerization of $[CO_2^{\bullet}]^-$ to $[C_2O_4]^{2-}$. Additionally, one of those insitu generated copper-coordination polynuclear complexes, is a mesoporous material and has shown interesting N_2 sorption properties. In a wide temperature range all the Cu polynuclear materials exhibits interesting semiconducting behavior. Constant research in this endeavor is under active progression in quest of advanced and effective transition metal polymerization catalysts for utilization of CO_2 like GHG.

Experimental

Materials

All solvents and chemicals used for synthesis were of analytical grade. Chemicals *e.g.;* benzaldehyde, 2,2′-bpy, 2-amino pyridine, salicylaldehyde were purchased from Spectrochem and used without further purification. 2-chloromethyl pyridine hydrochloride, 2-(2-pyridyl)ethylamine, triethyl amine are purchased from Aldrich. Analytical grade acetonitrile, benzonitrile, methanol, dichloromethane, DMF were purchased from Fluka and used without further purification. BOC make XL grade Argon and Carbon dioxide gas were used.

Instrumentation

A perkin Elmer 2400C elemental analyser was used to collect the microanalytical (C, H, N) data. UV-Vis spectroscopy was done on ALS SEC 2000 and Varian (Model Cary 100 Bio) spectrophotometer. IR spectra were carried out in a Perkin Elmer FT-IR spectrometer (spectrum 65) (Using KBR pellets). Powder X-ray diffraction (XRD) patterns of different complexes were analyzed with a Bruker D8 Advance X-ray diffractometer using Ni-filtered Cu Kα (λ= 0.15406 nm) radiation. N_2 adsorption/desorption isotherms of the complex was recorded at 77 K on a Quantachrome Autosorb-1-C. Prior to measurement, the samples were degassed at 373 K for 8 h under high vacuum conditions. Transmission electron microscopy (TEM) images of the mesoporous material were obtained using a JEOL JEM 2010 transmission electron microscope operating at 200 kV. The samples were prepared by dropping 2 μL of respective colloidal solution onto carbon-coated Copper grids. ESI-MS spectra were recorded on a micro mass Q-TOF mass spectrometer (serial no. YA 263), Advion compact mass spectrometer (serial number: 3013-0140) and FAB-MS (Jeol JMS700). Magnetic susceptibility measurements between 2-300 K were carried out in a SQUID magnetometer, MPMS Quantum Design Magnetometer, at the Unitat de Mesures Magnètiques (Universitat de Barcelona). Two different magnetic fields were used for the susceptibility measurements, 200 G (2-5 K) and 3000G (2-300 K), with superimposable graphs. Pascal's constants were used to estimate the diamagnetic corrections for the compounds. The fit was performed by minimizing the function $R = \Sigma[(\chi_M T)_{exp} - (\chi_M T)_{calc}]^2/\Sigma[(\chi_M T)_{exp}]^2$.

For electrical measurements the powder was taken in a steel mould of 1 cm diameter and compacted at a pressure of 5 tons/cm^2. Silver paint electrodes (supplied by Acheson Colloiden B.V., Holland) were applied on two opposite faces. Direct-current (dc) conductivity was measured by an 8 1/2 digit Agilent 3458A multimeter. The temperature dependence of conductivity was measured in a furnace with a Eurotherm 8502 temperature controller. The ac measurement was done by HP4902A Impedance Analyzer.

Syntheses of complexes

$[Cu(bpy)(C_2O_4)]_n$ (**1**): An equimolar mixture of bpy (156 mg, 1 mmol) and $CuCl_2$ (135 mg, 1 mmol) were dissolved in 50 mL methanol and the mixture was allowed to stir for 2 hours at room temperature. Initially a light green colored precipitate was developed, which on further addition of $AgClO_4$ (415 mg, 2 mmol) changes to intense blue along with a precipitate of AgCl. After removal of the solvent by evaporation under reduced pressure, the dry residue was taken in 50 mL benzonitrile solvent and transferred to a 100 mL capped glass stirrer vessel of Buchi miniclave steel. CO_2 gas purging during next ~ 0.5 h at room temperature was continued to produce light blue colored CO_2 inclusion polynuclear complex. This material on prolong staying inside an argon glove box fridge (-5°C) for ~12 h produce single crystals of $[Cu(bpy)(C_2O_4)]_n$ (**1**). Yield: 255 mg, 75%. Anal. calcd. for $C_{12}H_{12}N_2O_6Cu$: C, 41.88% ; H, 3.49% ; N, 8.14%. Found: C, 42. 05%; H, 3.36%; N,8.04%. Characteristic IR Peaks (KBr disk, υ, cm^{-1}) : 1652(s), 1089(br), 1447(s) , 773(s), 730(s), 626(s). UV/Vis peaks, λ_{max}, nm(ε, M^{-1} cm^{-1}): 215 (20550), 245 (12950), 300(14550), 700(25).

$[Cu(bpy)(PPh_3)_2]ClO_4$(1'): Under the same reaction condition as of complex **1,** during CO_2 purging for ~ 0.5 h at room temperature, excess PPh_3 (790 mg) was added to the solution mixture. Prolong standing of the crude product over 10 h in an argon blanketing atmosphere yielded X-Ray quality single crystals of $[Cu(bpy)(PPh_3)_2(ClO_4)]$ (**1'**) in reasonably good yield along with less proportion of complex **1**. Yield: 531 mg, 63%. Anal. calcd. for $C_{46}H_{38}CuN_2P_2ClO_4$: C, 65.42% ; H, 4.50% ; N, 3.31%. Found: C, 65.37%; H, 4.43%; N,3.41%. Characteristic IR Peaks (KBr disk, υ, cm^{-1}): 1593(s), 1480(s), 1437 (s), 1092(s), 747(s), 695(s), 622(s), 514(s), 488(s). UV/Vis peaks, λ_{max}, nm(ε, M^{-1} cm^{-1}): 240(25060), 400(3154).

$[Cu(2\text{-}AMP)_2(C_2O_4)]_n$ (**2**): **L^1** (276 mg, 1 mmol) and $CuCl_2$ (135 mg, 1 mmol) in presence of NEt_3 (280 μL, 2mmol) were dissolved in 50 mL benzonitrile and allowed to stir for 1 hour at room temperature. The reaction mixture was transferred to a 100 mL capped glass stirrer vessel of Buchi miniclave steel and concomitant CO_2 purging during ~0.5 h produces a light green colored crude product. X-Ray quality single crystals were obtained from a concentrated solution of benzonitrile at -5°C**.** Yield: 245 mg, 72%. Anal. calcd. for $C_{12}H_{12}N_4O_4Cu$: C, 42.38%; H, 3.53%, N, 16.48%. Found: C, 42.28%; H, 3.48%, N, 16.42%. Characteristic IR Peaks (KBr disk, υ, cm^{-1}): 1664(s), 1632(s), 1594(s), 1566(s), 1497(s), 1452(s), 1311(s), 1263(s), 1167(s), 796(s), 763(s). UV/Vis peaks, λ_{max}, nm(ε, M^{-1} cm^{-1}): 280(11100), 310(10210).

$[Cu(L^2)(Cl)]$ (**3**): Room temperature reaction of $CuCl_2$ (135 mg, 1 mmol) and **L^2** (320 mg, 1 mmol) in presence of NEt_3 (140 μL, 1mmol) in 50 mL MeOH with constant stirring for 3 hour produces complex **3**. Slow evaporation of solution mixture at room temperature yields single crystals of complex **3** suitable for X-Ray study. Yield: 488 mg, 90%. Anal. Calcd. for $C_{20}H_{20}N_3OCuCl.(7H_2O)$:C, 44.16% ; H, 6.25% ; N, 7.73%. Found: C, 43.97%; H, 5.97%; N, 7.62%. Characteristic IR Peaks (KBr disk,υ, cm^{-1}) : 1609(s), 1484(s), 1450(s) , 1110(s), 1031(s), 767(s). UV/Vis peaks, λ_{max}, nm(ε, M^{-1} cm^{-1}): 215(19000), 260(19850), 600(9).

Complex (**4**): Complex **3** (543 mg, 1 mmol) was taken in 50 mL benzonitrile inside a glass stirrer vessel of Buchi miniclave steel and CO_2 purging during ~0.5 h forms greenish blue crude product. The microcrystalline complex **4** were obtained by recrystallization from benzonitrile solution. Unfortunately X-Ray quality single crystals were not obtained. Yield: 554 mg, 69%. Anal. Calcd. for $C_{34}H_{34}N_7O_4Cu_2Cl_2$: C, 51.06% ; H, 4.25% ; N, 12.26%. Found: C, 50.95%; H, 4.30%; N, 12.39%. Characteristic IR Peaks (KBr disk, υ, cm^{-1}) : 1633(s), 1609(s), 1451(s), 1157(s), 1021(s) , 763(s). UV/Vis peaks, λ_{max}, nm(ε, M^{-1} cm^{-1}): 205(23500), 260(12600), 600(20).

X-Ray Structure Determination

Crystallographic data for the complexes **1**, **1'**, **2**, **3** and **L^1** are collected in Table S1-S5 in ESI†. All data were collected on a Bruker SMART Apex-II diffractometer equipped with graphite

monochromated Mo Kα radiation (λ = 0.71073 Å). Corrections were done for Lorentz-polarization effects.

For complex **1**: A total of 6459 reflections were collected, out of which 2417 were unique (R_{int} = 0.028), satisfying the ($I > 2\sigma(I)$) criterion, and were used in subsequent analysis.

For complex **1'**: A total of 29280 reflections were collected, out of which 6423 were unique (R_{int} = 0.056), satisfying the ($I > 2\sigma(I)$) criterion, and were used in subsequent analysis.

For complex **2**: A total of 6866 reflections were collected out of which 1171 were unique (R_{int} = 0.024), satisfying the ($I > 2\sigma(I)$) criterion, and were used in subsequent analysis.

For complex **3**: A total of 15481 reflections were collected out of which 4042 were unique (R_{int} = 0.064), satisfying the ($I > 2\sigma(I)$) criterion, and were used in subsequent analysis. There were disorders in the solvent water molecules in the crystals. We have masked them by a solvent masking procedure (here SQUEEZE). The details are given in the SQUEEZE details of complex **3** cif (See ESI†, Fig. S6b: for further details about masked solvent molecules by Thermogravimetric analysis profile).

For ligand $\mathbf{L^1}$: A total of 10933 reflections were collected out of which 2813 were unique (R_{int} = 0.032), satisfying the ($I > 2\sigma(I)$) criterion, and were used in subsequent analysis.

All the structures were solved by employing the SHELXS-97 program package and were refined by full-matrix least-squares based on F^2 (SHELXL-97).[27, 28] All the hydrogen atoms were added in calculated positions. All calculations are carried out using PLATON[29] and WinGX system.[30]

Acknowledgements

Financial support received from CSIR-CMERI initial start up grant (OLP 182112) and DST Fast Track Project for young researchers (GAP 183112) are gratefully acknowledged. P.B is thankful to Dr. Pijush Pal Roy, Director, CSIR-CMERI for his immense support to carry out this work in CSIR-CMERI. Dr. Sasankasekhar Mohanta, CU is gratefully acknowledged for many helpful discussions. Corbella is thankful to Ministerio de economia y Competitividad of Spain through the project CTQ2012-30662 and the ComissióInterdepartamental de RecercaiInnovacióTecnològica of la Generalitat de Catalunya (CIRIT) (2009-SGR1454). Reviewers are also gratefully acknowledged for many insightful suggestions.

Notes and references

[a] *Surface Engineering & Tribology Group, CSIR-Central Mechanical Engineering Research Institute, Mahatma Gandhi Avenue, Durgapur 713209, India. Fax: +91-343- 2546 745; Tel: +91-343-6452220; E-mail: pr_banerjee@cmeri.res.in, priyabrata_banerjee@yahoo.co.in*

b Academy of Scientific & Innovative Research, CSIR-Central Mechanical Engineering Research Institute, Mahatma Gandhi Avenue, Durgapur 713209, India

[c] *Departament de Química Inorgànica and Institut de Nanociència i Nanotecnologia (INIUB), Universitat de Barcelona. Martí i Franquès 1-11, 08028-Barcelona, Spain. Fax: 34934907725.*

[d] *Indian Association for the Cultivation of Science, Jadavpur, Kolkata – 700 032, India.*

[e] *School of Basic Science, IIT Indore, India.*

[f] National Institute of Technology, *Mahatma Gandhi Avenue, Durgapur 713209,* West Bengal, India.

† Electronic Supplementary Information (ESI) available: [Crystallographic detalis and ORTEP diagram of **1**, **1'**, **2**, **3** and $\mathbf{L^1}$, ESI and FAB-MS data, CHN analysis, FT-IR, UV-Vis data for all the compounds are included in supporting information.]

See DOI: 10.1039/b000000x/

CCDC: 1002488, 1002489, 1002490, 990722, 981596 for **1**, **2**, **3**, $\mathbf{L^1}$ and **1′**.

1 (a) J. Costamagna, G. Ferraudi, J. Canales and J. Vargas; *Coord. Chem. Rev.*, 1996, **148**, 221; (b) Carbon dioxide as a source of carbon biochemical and chemical uses M. Aresta and G. Forti, *Nato ASI Series, Series C : Mathematical and Physical Sciences*, 206; (c) A. Behr, *Carbon Dioxide Activation by Metal Complexes*; VCH: Weinheim, Germany, 1988.

2 M. Jitaru, *J. Appl. Elec. Chem.*, 1997, **27**, 875.

3 M. Rudolph, S. Dautz, E-G. Jäger, *J. Am. Chem. Soc.*, 2000, **122**, 10821.

4 J. P. Collin and J. P. Sauvage, *Coord. Chem. Rev.*, 1989, **93**, 245.

5 A. Gennaro, A. A. Isse, J-M Saveant, M-G Severin and E. Vianello, *J. Am. Chem. Soc.*, 1996, **118**, 7190.

6 (a) R. Angamuthu, P. Byers, M. Lutz, A. L. Spek and E. Bouwman, *Science*, 2010, **327**, 313; (b) M. K. Bhunia, S. K. Das, M. M. Seikh, K. V. Domasevitch and A. Bhaumik, *Polyhedron,* 2011, **30**, 2218.

7 I. Iriepa, A. Lorente, E. Galvez, P. Rubio, F. Florencio, S. Garcia-Blanco, *J. Mol. Struc.,*1986, **142**, 443.

8 (a) C. M. S-Hauser, K. Mereiter, R. Schmid and K. Kirchner *Eur. J. Inorg. Chem.*, 2003, 1883; (b) C. M. S-Hauser, K. Mereiter, R. Schmid and K. Kirchner, *Organometallics,* 2002*,* **21***,* 4891.

9 (a) H. Adams, N. A. Bailey, C. O. Rodriguez de Barbarin, D. E. Fenton and Q-Y. He, *J. Chem. Soc. Dalton Trans.,*1995, 2323. (b) S. –G. Kang, S. –J. Kimand and J. H. Jeong, Polyhedron, 1998, **17**, 3227.

10 (a) D. Chandra and A. Bhaumik, *J. Mater.*Chem., 2009, **19**, 1901; (b) S. K. Das, M. K. Bhunia, Md. M. Seikh, S. Dutta and A. Bhaumik, *Dalton Trans*, 2011, **40**, 2932.

11 A. W. Addison, T. N. Rao, J. Reedijk, J. V.Rijn and G. C.Verschoor, *J. Chem. Soc., Dalton Trans.* 1984, 1349.

12 (a) A. Wladimirsky, D. Palacios, M. C. D'Antonio, A. C. González-Baró and E.J. Baran, *The Journal of the Argentine Chemical Society*, 2011, **98**, 71. (b) K. Tanaka,Y. Kushi, K. Tsuge, K. Toyohara, T. Nishioka and K. Isobe, *Inorg. Chem.*, 1998, **37**, 120.

13 (a) R. Valliulin, S. Naumov, P. Galvosas, J. Karger, H. –j. Woo, F. Porcheron and P. A. Monson, *Nature, 2006,* **443***,* 965. (b) H. Yang, F. Wang, Y. Kang, T-H. Li and J. Zhang, *Dalton Trans.*, 2012, **41**, 2873.

14 (a) A. P. Wight and M. E. Davis, *Chem. Rev.*, 2002, **102**, 3589; (b) A. Sayari, S. Hamoudi and Y. Yang, *Chem. Mater.*, 2005, **17**, 212; (c) A. Taguchi and F. Schuth, *Microporous Mesoporous Mater.*, 2005, **77**, 1; (d) D. Chandra, M. W. Kasture and A. Bhaumik, *Microporous Mesoporous Mater.*, 2008, **116**, 204.

15 S. K. Das, M. K. Bhunia and A. Bhaumik, *Dalton Trans.,* 2010, **39**, 4382.

16 G. A. Baker and G. S. Rushbrooke, *Phys. Rev.,* 1964, **135**, 1272.

17 O. Kahn and M. F. Charlot, *Nouv. J. Chim.*, 1980, **4**, 567.

18 H. Oshio and U. Nagashima, *Inorg. Chem.*, 1992, **31**, 3295.

19 O. Castillo, A. Luque, P. Román, F. Lloret and M. Julve, *Inorg. Chem.,* 2001**, 40**, 5526.

20 J. Suárez-Varela, J. M. Domínguez-Vera, E. Colacio, J. C. Ávila-Rosón, M. A. Hidalgo and D. Martín-Ramos, *J. Chem. Soc., Dalton Trans.,* 1995, 2143.

21 O. Castillo, A. Luque, F. Lloret and P. Román, *Inorg. Chim. Acta.*, 2001, **324**, 141.

22 R. S. Vilela, T. L. Oliveira, F. T. Martins, J. A. Ellena, F. Lloret, M. Julve and D. Cangussu, *C. R. Chimie.*, 2012, **15**, 856.

23 I. Castro, J. Faus, M. Mollar, A. Monge and E. Gutiérrez-Puebla, *Inorg. Chim. Acta.,* 1989, **161**, 97.

24 M. L. Calatayud, I. Castro, J. Sletten, F. Lloret and M. Julve, *Inorg. Chim. Acta*., 2000, **300**–**302**, 846.

25 D. Cangussu, H. O. Stumpf, H. Adams, J. A. Thomas, F. Lloret and M. Julve, *Inorg. Chim. Acta*., 2005, **358**, 2292.

26 J. C. Bonner and M. E. Fisher, *Phys. Rev. A*., 1964, **135**, 640.

27 G. M. Sheldrick, *Acta. Crystallogr. Sec. A.,* 1990, **46**, 467.

28 G. M. Sheldrick, SHELXL 97; University of Gottingen; Gottingen, Germany, 1997.

29 A. L. Spek, *J. Appl. Cryst*., 2003, **36**, 7.

30 L. J. Farrugia, WinGX-A Windows Program for crystal structure analysis., *J. Appl. Crystallogr.,* 1999, **32**, 837.

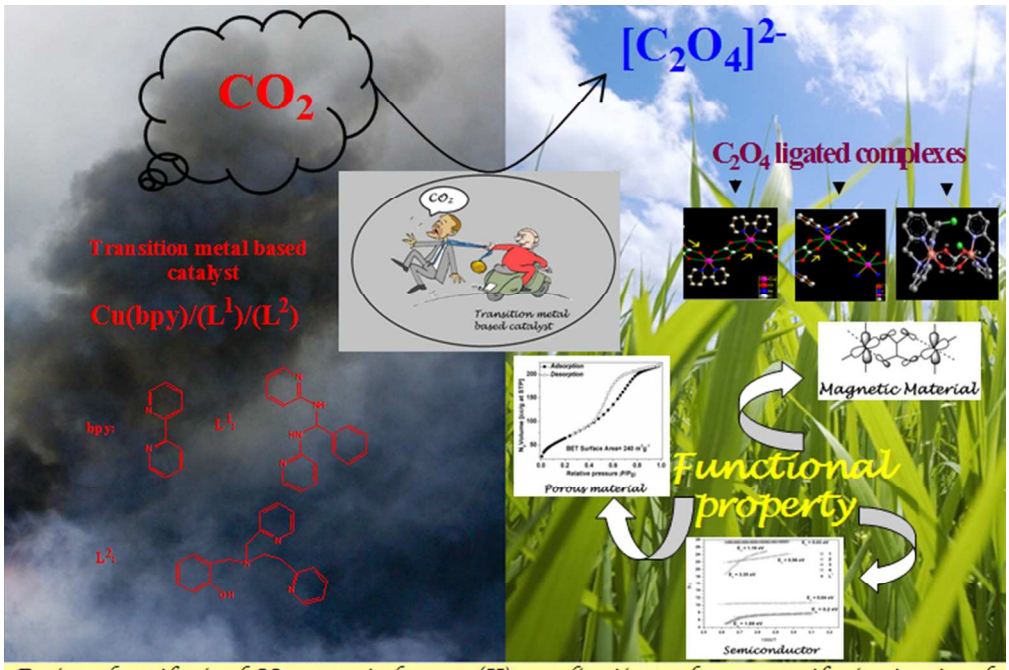

Designed synthesis of CO_2 promoted copper(II) coordination polymers: synthesis, structural, spectroscopic characterization and versatile functional property studies†

Pritam Ghosh,[a] Additi Roychowdhury,[ab] Montserrat Corbella,[c] Asim Bhaumik,[d] Partha Mitra,[d] Shaikh M. Mobin,[e] Ayan Mukherjee,[f] Soumen Basu,[f] and Priyabrata Banerjee*[ab]

196x151mm (96 x 96 DPI)